# Modeling and control of a cable-suspended robot for inspection of vertical structures

**Nicole Barry, Erin Fisher, and Joshua Vaughan**

Department of Mechanical Engineering, University of Louisiana at Lafayette, Lafayette, LA 70504, USA

E-mail: joshua.vaughan@louisiana.edu

**Abstract.** In this paper, a cable-driven system is examined for the application of inspection of large, vertical-walled structures such as chemical storage tanks, large ship hulls, and high-rise buildings. Such cable-driven systems are not commonly used for these tasks due to vibration, which decreases inspection accuracy and degrades safety. The flexible nature of the cables make them difficult to control. In this paper, input shaping is implemented on a cable-driven system to reduce vibration. To design the input shapers, a model of the cable-driven system was developed. Analysis of the dominant dynamics and changes in them over the large workspace are also presented. The performance improvements provided by the input shaping controller are quantified through a series of simulations.

## 1. Introduction

A cable-driven parallel manipulator (CDPM) is a type of parallel manipulator in which each cable in the mechanism is connected to the end-effector in parallel with the other cables. As opposed to a serial manipulator (*e.g.* robotic arm), each cable is actuated independently of the others. Sometimes called cable-direct-driven robots, these systems are currently being studied and implemented in a variety of applications due to the fact that cables have a high load capacity, low mass, and thus lower cost than the traditional serial manipulator [1, 2]. In addition, a CDPM can have a large workspace by varying cable lengths or attaching the winches to mobile bases. This allows for inspection robots to reach hazardous environments and be transported easily [3–8].

Currently, cable-driven parallel manipulators include the SkyCam [9], used to video sporting events, and SPIDAR [10], used as a means of interacting with a virtual reality. In these cases and most others, the CDPMs are redundantly restrained, meaning that they have more driven cables than the number of degrees of freedom. This is done to improve the stability of the system and is largely motivated by the fact that cables are flexible in nature and only capable of being driven in one direction via tension. In contrast, this paper will investigate an incompletely restrained cable-driven system with two cables and three degrees of freedom.

Cable-driven parallel manipulators have been implemented for inspecting and cleaning of vertical structures [11, 12]. The designs thus far primarily rely on the mechanical hardware to limit vibration of the mechanism. Commonly, vertical structures are inspected for damages manually, compromising accuracy and leading to long inspection times. For example, the inspection robot SAM is held in tension on both the top and bottom of a high-rise building

**Figure 1:** Vertical, Double-Wall Aboveground Storage Tanks [15]

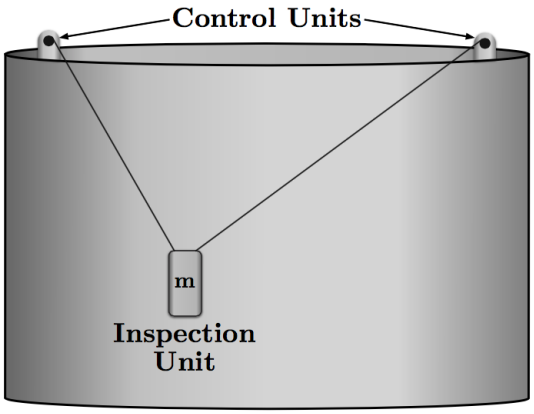


**Figure 2:** Sketch of a CDPM Tank Inspection System

while the robot is simply controlled by an operator to maneuver up or down [11]. The process is inefficient, and only a small portion of the building can be inspected per pass of the robot.

Focusing on cylindrical vertical structures, specifically single- and double-walled aboveground storage tanks like those shown in Figure 1, this paper aims to begin the work of applying CDPMs for the inspection of structures with complex geometries. Currently, the Code of Federal Regulations mandates that all aboveground storage tanks be inspected within the regulations given by API 650, API 653, and STI SP001 standards [13]. There are two types of inspections required by the standards: formal and informal. The informal visual inspection is required to take place frequently, usually monthly, while a formal, more-thorough, inspection is scheduled and performed by authorized personnel. The scheduled inspection depends on the type of tank, use of the tank, and its environment but is typically completed every 1–3 years. Not only is it important that the tanks be monitored visually, but it is also important that accurate knowledge of the condition of the tanks be acquired and recorded. Poor conditions of the tank may result from paint failures, pitting, corrosion, weld thinning, and leaks in seams or rivets [13]. While a visual inspection can determine the obvious damage, precise inspection instruments may be beneficial for understanding the lifespan of the tank. A case of avoidable tank leakage led to a spill into the Elk River in West Virginia, leaving thousands of people with unclean water [14]. A robotic system, like the one sketched in Figure 2, is one possible way to improve the inspection of cylindrical tanks and help prevent such disasters.

The paper will explore the use of a cable-driven parallel manipulator for the inspection of cylindrical structures. First, a preliminary model and dynamics for a cable-driven system consisting of two moveable winches and a payload, all moving along the shell of a cylindrical storage tank, is presented. In Section 2, the changes in natural frequency due to nonlinearities of the system are specified. Section 3 introduces Input Shaping to be used in the nearly-linear region of the workspace in order to reduce the payload vibration, making the system more efficient and safe. Multiple input shapers are applied and compared. Finally, conclusions are presented in Section 4.

## 2. System Dynamics

In order to accurately represent the cable-driven inspection system, a complex model must be created, consisting of two control-unit winches adhered to the wall of an aboveground storage tank driving an inspection unit, like that shown in Figure 2. The winches, responsible for

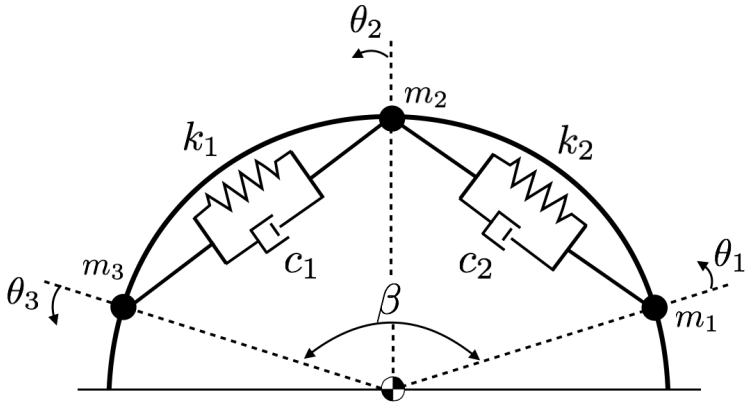


**Figure 3:** Simplified Planar Model

movement of the inspection unit, move around the shell of the tank. This motion of the winches on the cylindrical shell, along with retraction or extension of their cables, move the inspection unit payload.

As an intermediate step in fully representing the system dynamics, a planar model of the system from the top view was created and is shown in Figure 3. The simplification does not account for three-dimensional pendulum affect of the cable-suspended inspection unit payload, but does include the motion of the payload along the curvature of the cylindrical structure. The masses of the winches, $m_1$ and $m_3$, along with the mass of the payload, $m_2$, are all fixed along a circle, representing the outer shell of the cylindrical tank. The equations of motion describing the system are:

$$\ddot{\theta}_1 = -\frac{1}{2m_1}\delta_{11}c_1(\dot{\theta}_1 - \dot{\theta}_2) - \frac{k_1}{m_1}\sin(\theta_1 - \theta_2) \tag{1}$$

$$\ddot{\theta}_2 = -\frac{1}{2m_2}\left[\delta_{21}c_1(\dot{\theta}_2 - \dot{\theta}_1) + \delta_{22}c_2(\dot{\theta}_2 - \dot{\theta}_3)\right] - \frac{k_1}{m_2}\sin(\theta_2 - \theta_1) - \frac{k_2}{m_2}\sin(\theta_2 - \theta_3) \tag{2}$$

$$\ddot{\theta}_3 = -\frac{1}{2m_3}\delta_{33}c_2(\dot{\theta}_3 - \dot{\theta}_2) - \frac{k_2}{m_3}\sin(\theta_3 - \theta_2) \tag{3}$$

where the corresponding $\delta_{ij}$ terms can be described by the following equations:

$$\delta_{11} = \frac{\sin^2(\theta_1 - \theta_2)}{1 - \cos(\theta_1 - \theta_2)} \qquad \delta_{21} = \frac{\sin^2(\theta_2 - \theta_1)}{1 - \cos(\theta_2 - \theta_1)} \tag{4}$$

$$\delta_{22} = \frac{\sin^2(\theta_2 - \theta_3)}{1 - \cos(\theta_2 - \theta_3)} \qquad \delta_{33} = \frac{\sin^2(\theta_3 - \theta_2)}{1 - \cos(\theta_3 - \theta_2)} \tag{5}$$

Angles $\theta_1$, $\theta_2$, and $\theta_3$ correspond to the movement of each mass from the system equilibrium. For the simulations presented in this paper, the masses, $m_1$, $m_2$, and $m_3$ are 2.5 kg, 10 kg, and 2.5 kg, respectively. The spring constants, $k_1$ and $k_2$, are both 100 N/m. The parameters were chosen relative to one another in order to simulate a possible real system.

In order to simulate the response of the inspection unit payload, $m_1$ and $m_3$ were given bang-coast-bang acceleration inputs, reducing the system to one mode of vibration. Figure 4 shows the payload's response to the acceleration inputs. With a maximum acceleration of 20 rad/s$^2$ and maximum velocity of 2 rad/s, $m_1$ and $m_3$ move to a final position of 20°. The residual

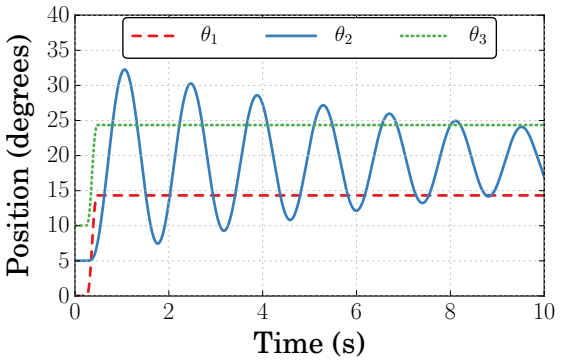


**Figure 4:** Payload's Response to Bang-Coast-Bang Acceleration Input

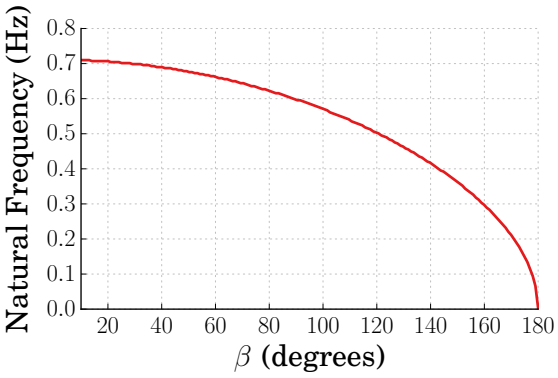


**Figure 5:** Changes in Natural Frequency as a Function of Winch Spread

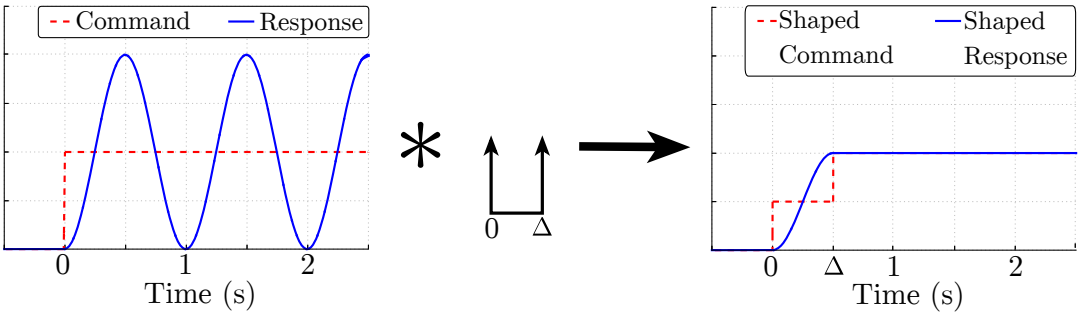


**Figure 6:** The Input Shaping Process

vibration of $m_2$ due to the acceleration input is significant, and it would likely be unsafe and inefficient to use the system.

The spread of the winches, represented as angle $\beta$, is defined by the angle between $m_1$ and $m_3$. At each angle of spread, the system frequency was estimated around the static equilibrium utlizing the Fast Fourier Transform (FFT). Figure 5 plots the changes in natural frequency as a function of $\beta$. The natural frequency remains nearly constant between $\beta = 10°$ and $40°$. Over this range of angles, the natural frequency is only 0.0315 Hz, or $\pm 2.25\%$, from the average frequency over the range, 0.697 Hz. In other words, within this region of the workspace, natural frequency is nearly constant.

## 3. Input Shaping

Input shaping, commonly used for crane control [16–18], is one possible control method for reducing vibration of the cable-driven system. To date, input shaping has only been implemented on CDPMs moving along a flat surface [20, 21].

An input shaper consists of a series of impulses designed to reduce vibration at or around the system's natural frequencies and damping ratios. To implement input shaping, the original command is convolved with the series of impulses, creating a new, input-shaped command to be sent to the system. If the input shaper is properly designed, then the new, shaped command results in a response in which the residual vibration is reduced or eliminated. This is demonstrated in Figure 6; the original command is convolved with a two-impulse shaper reducing the vibration to zero and increasing the length of the command by the duration of the shaper.

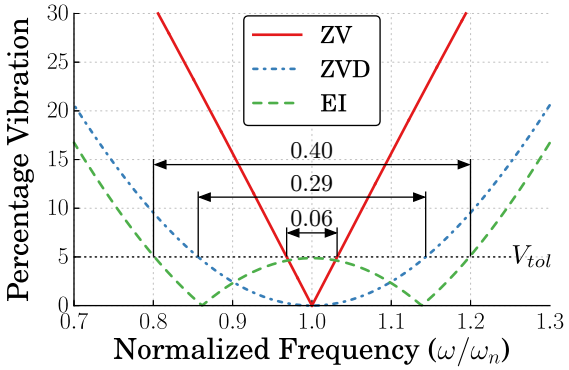


**Figure 7:** Sensitivity Plot for Multiple Input Shapers

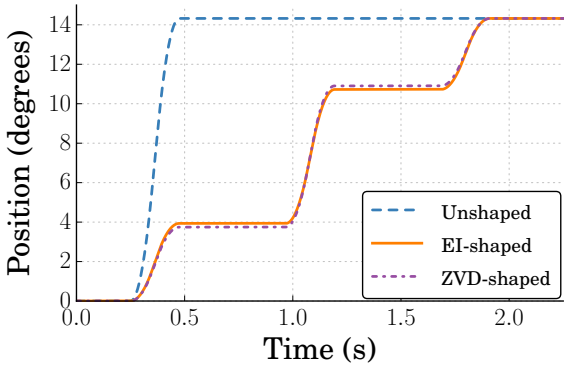


**Figure 8:** Resulting $m_1$ Motion from Shaped Bang-coast-Bang Input

The shaper used in the illustrative example response in Figure 6 was the well-known the Zero-Vibration (ZV) shaper. The ZV Shaper is designed to reduce residual vibration to zero, but only at the design natural frequency and damping ratio [19]. To account for the nonlinearities or modeling errors, robustness to frequency changes can be included in the input shaper design process. For example, the Extra Insensitivity (EI) shaper was designed to increase robustness by allowing for some small, tolerable level of vibration at the design frequency [17]. The Zero Vibration and Derivative (ZVD) shaper provides robustness around the design frequency by not only limiting the vibration to zero at the design frequency, but also the limiting derivative of the function describing it to zero, as well [19].

The sensitivity curve plot in Figure 7 compares the robustness of the ZV, ZVD, and EI shapers. The sensitivity curve shows how the vibration resulting from a command shaped by an input shaper varies as the natural frequency of the system deviates from the one for which the shaper was designed. It is a portrait of the shaper's robustness to changes in frequency. To quantify this robustness, Insensitivity is used. The Insensitivity of a shaper is defined as the range of normalized frequency for which the vibration is reduced to below some tolerable level, typically 5% of the unshaped vibration. For example, the Insensitivity of the EI shaper at a tolerable level of vibration of 5% is $I(5\%) = 0.40$. This is the highest of the three shapers shown in Figure 9, making it the most robust shaper of the three. Although robustness is desirable, shaper duration increases with robustness, making it important to consider the tradeoff during input shaper selection [17–19].

If the commands used to create the response shown in Figure 4 are shaped with a ZVD or EI shaper, the resulting motion of $m_1$ is shown in Figure 8 (Mass $m_3$ follows an identical profile,

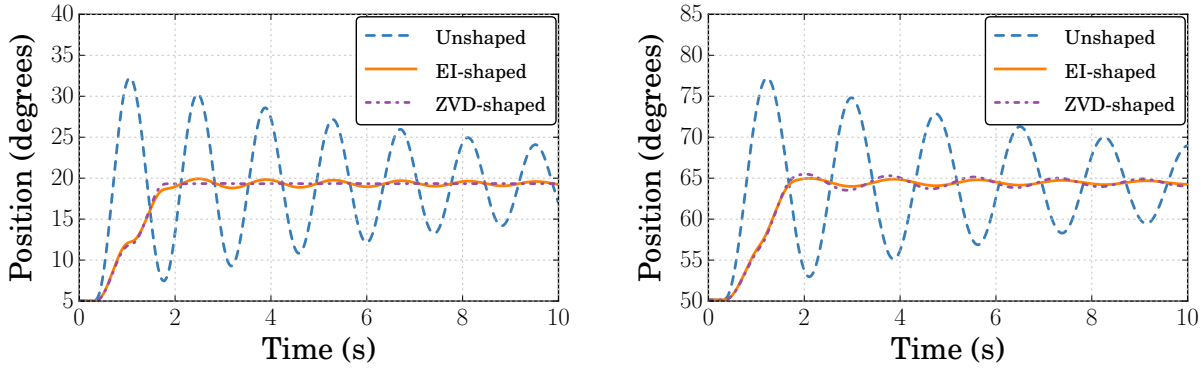


**(a)** Responses for Winch Spread of 10° **(b)** Responses for Winch Spread of 100°

**Figure 9:** Comparison of Unshaped, ZVD, and EI Shaped Responses

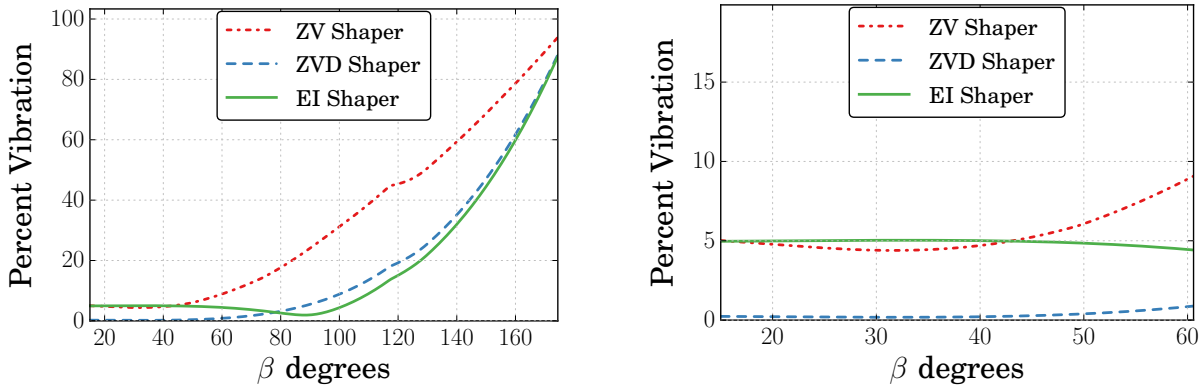


**(a)** All Examined Winch Spreads **(b)** Nearly-Constant-Frequency Winch Spread

**Figure 10:** Percentage Vibration over a Range of Winch Spreads

just offset from $m_1$ bye the winch spread, $\beta$.). Both shapers increase the command duration beyond the unshaped case. However, the commands result in responses with much less vibration than the unshaped case, as shown in Figure 9, which shows the payload responses to the the ZVD- and EI-shaped bang-coast-bang inputs, along with unshaped response for comparison.

Figure 9a shows the shaped response with a winch spread of 10°, contained within the region of nearly-constant natural frequency of 0.697 Hz. Figure 9b shows the response of a similar move, but for a winch spread of 100°. The vibration is slightly larger than that with the narrower winch spread. At this angle of winch spread, the natural frequency has decreased to 0.54 Hz. This represents an approximate 22% decrease in frequency from that which the two shapers were designed for, leading to the increased vibration. However, both shaped cases still result in a residual vibration that is dramatically less than that from the unshaped case.

In Figure 10a, the vibration amplitude of the shaped response as a percentage of the vibration of the unshaped response, or the percent vibration, of each shaper is compared over a range of $\beta$ from 15° to 170°. The ZVD shaper generates the lowest percentage of vibration within the operating range, while the EI shaper results in the lowest average percent vibration. Within the complete range of winch spreads, from 15° to 180°, the percent vibration is never as great as the unshaped case. Figure 10b more closely plots the same data, within the range of likely winch spreads. In this range, as seen earlier in Section 2, the natural frequency is nearly constant. As a result, all shapers remain at or below 5% vibration for winch spreads up to 35°. Due to

their robustness, the ZVD and EI shapers limit vibration to below 5% of that present in the unshaped case over the entire range of winch spreads shown in this plot.

## 4. Conclusion

This paper presented a method for control of cable-driven parallel manipulators designed to inspect the shell of cylindrical structures, such as aboveground storage tanks. A planar model of the top view of a tank was simulated in order to gain knowledge of the dynamics of the system. Limitations for the winch spread were determined by defining the region in which the natural frequency of the system is nearly constant. Within the specified linear region, ZV, ZVD, and EI input shapers were compared via residual vibration amplitude, showing that all reduce vibration from the unshaped case. Within the entire winch spread reviewed, from 10° to 180°, the vibration of the shaped response was always lower than that of the unshaped response.

## References

[1] R. L. W. Ii, "Planar Translational Cable-Direct-Driven Robots," *Journal of Robotic Systems*, vol. 20, no. 3, pp. 107–120, 2003.
[2] Y. Li and Q. Xu, "GA-Based Multi-Objective Optimal Design of a Planar 3-DOF Cable-Driven Parallel Manipulator," *IEEE International Conference on Robotics and Biomimetics, 2006. ROBIO '06.*, pp. 1360–1365, December 2006.
[3] P. Bosscher and I. Ebert-Uphoff, "Wrench-based analysis of cable-driven robots," *IEEE International Conference on Robotics and Automation, 2004. Proceedings. ICRA '04. 2004*, vol. 5, no. April, pp. 4950–4955, 2004.
[4] W. T. S. K. Kawamura, S. Choe, "Devlopment of an Ultrahigh Speed Robot FALCON using Wire Drive System," *Wire*, vol. 1, pp. 215–220, May 1995.
[5] O. M. O. Ma and X. D. X. Diao, "Dynamics analysis of a cable-driven parallel manipulator for hardware-in-the-loop dynamic simulation," *Proceedings, 2005 IEEE/ASME International Conference on Advanced Intelligent Mechatronics.*, pp. 837–842, July 2005.
[6] C. B. Pham and S. H. Yeo, "Workspace Analysis and Optimal Design of Cable-Driven Parallel Manipulators," *Conference of Robotics, Automation, and Mechatronics*, vol. 1, pp. 219–224, December 2004.
[7] R. L. Williams II and P. Gallina, "Planar Cable-Direct-Driven Robots, Part I: Kinematics and Statics," *2001 ASME Design Technical Conference*, no. 740, pp. 1–9, 2001.
[8] R. Yao, X. Tang, J. Wang, and P. Huang, "Dimensional Optimization Design of the Four-Cable-Driven Parallel Manipulator in FAST," *IEEE/ASME Transactions On Mechatronics*, vol. 15, no. 6, pp. 932–941, 2010.
[9] R. R. Thompson and M. S. Blackstone, "Three-Dimensional Moving Camera Assembly with an Informational Cover Housing." US Patent 6873355 B1, March 2005.
[10] L. Liu, S. Miyake, K. Akahane, and M. Sato, "Development of String-based Multi-finger Haptic Interface SPIDAR-MF," in *International Conference on Artificial Reality and Telexistence (ICAT)*, (Tokyo, Japan), pp. 67–71, 2013.
[11] J. Sobotka, "Building inspection device," Sept. 12 2013. US Patent App. 13/884,157.
[12] D. Sun, J. Zhu, and S. K. Tso, "A climbing robot for cleaning glass surface with motion planning and visual sensing," *Climbing & Walking Robots, Towards New Applications, Book edited by Houxiang Zhang, ISBN 978-3-902613-16-5*, no. October, pp. 221–234, 2007.
[13] A. P. Institute, "API 653: Tank Inspection, Repair, Alteration, and Reconstruction," vol. 552.
[14] U. C. S. Board, "Csb investigation finds no record of inspections on freedom industries chemical storage tanks; leak in bottom of tank that contaminated charleston, wv, drinking water resulted from corrosion caused by water seeping through holes in tank roof."
[15] I. Highland Tank Manufacturing Company, "Aboveground vertical double-wall ul-142."
[16] K. L. Sorensen, W. Singhose, and S. Dickerson, "A controller enabling precise positioning and sway reduction in bridge and gantry cranes," *Control Engineering Practice*, vol. 15, no. 7, pp. 825–837, 2007.
[17] W. Singhose, W. Seering, and N. Singer, "Residual Vibration Reduction Using Vector Diagrams to Generate Shaped Inputs," *Journal of Mechanical Design*, vol. 116, no. 2, p. 654, 1994.
[18] J. Vaughan, A. Yano, and W. Singhose, "Comparison of robust input shapers," *Journal of Sound and Vibration*, vol. 315, no. 4-5, pp. 797–815, 2008.
[19] N. C. Singer and W. P. Seering, "Preshaping Command Inputs to Reduce System."

[20] J. Huey and W. Singhose, "Pendulum : Impact on Input Shaping," *Proceedings of 2003 IEEE Conference on Control Applications, 2003. CCA 2003.*, vol. 1, pp. 532–537, June 2003.
[21] J. R. Huey and W. Singhose, "Input Shaping Algorithm," in *7th International Conference on Motion and Vibration Control*, pp. 1–10, 2004.